

UC Office of the President

Recent Work

Title

A synthetic macromolecule for sentinel node detection: (99m)Tc-DTPA-mannosyl-dextran.

Permalink

<https://escholarship.org/uc/item/2mb748kv>

Journal

Journal of Nuclear Medicine, 42(6)

Authors

Vera, D R
Wallace, A M
Hoh, C
[et al.](#)

Publication Date

2001-06-01

Peer reviewed

A Synthetic Macromolecule for Sentinel Node Detection: ^{99m}Tc -DTPA-Mannosyl-Dextran

David R. Vera, Anne M. Wallace, Carl K. Hoh, and Robert F. Mattrey

Departments of Radiology and Surgery and UCSD Cancer Center, University of California, San Diego, La Jolla, California

We report the synthesis and preliminary biologic testing of a synthetic macromolecule, ^{99m}Tc -diethylenetriaminepentaacetic acid (DTPA)-mannosyl-dextran, for sentinel node detection.

Methods: Synthesis started with a 2-step process that attaches a high density of amino-terminated leashes to a dextran backbone. Allyl-bromide was reacted with pharmaceutical-grade dextran to yield allyl-dextran. After diafiltration with water, filtration, and lyophilization, the product was reacted with aminoethanethiol and ammonium persulfate. The resulting amino-conjugated dextran was dialyzed, filtered, and lyophilized. The mixed anhydride method was used to attach DTPA; after dialysis, filtration, and lyophilization, 2-imino-2-methoxyethyl-1-D-mannose was used to attach the receptor substrate. The molecular diameter was measured by dynamic light scattering. Amino, mannose, and DTPA densities were measured by trinitrobenzene sulfonate assay, sulfuric acid/phenol assay, and inductively coupled plasma spectroscopy of gadolinium-DTPA-mannosyl-dextran, respectively. Receptor affinity was measured by Scatchard assay of rabbit liver. Axillary, popliteal, and iliac lymph nodes and each injection site were assayed for radioactivity at 1 and 3 h after injection of approximately 3.7 MBq (0.050 mL) ^{99m}Tc -DTPA-mannosyl-dextran (0.22 nmol) or filtered ^{99m}Tc -sulfur colloid into the foot pads. Four animals were studied at each time point. **Results:** DTPA-mannosyl-dextran had a molecular weight of 35,800 g/mol and a molecular diameter of 7.1 nm. The final amine, mannose, and DTPA densities were 23, 55, and 8 mol per dextran. Labeling yields were in excess of 98% and stable for 6 h. Specific activities of 74×10^6 GBq/mol were achieved. The equilibrium dissociation constant for binding to the mannose-terminated glycoprotein receptor was 0.12 ± 0.07 nmol/L. The popliteal extraction at both 1 h and 3 h was significantly ($P < 0.05$) higher for ^{99m}Tc -DTPA-mannosyl-dextran ($90.1\% \pm 10.7\%$ and $97.7\% \pm 2.0\%$, respectively) than for filtered ^{99m}Tc -sulfur colloid (78.8 ± 6.5 and $67.4\% \pm 26.8\%$, respectively). ^{99m}Tc -DTPA-mannosyl-dextran exhibited significantly faster injection site clearance than did filtered ^{99m}Tc -sulfur colloid. The ^{99m}Tc -DTPA-mannosyl-dextran percentage injected dose (%ID) for the front and rear paws was 52.6 ± 10.5 and 52.3 ± 8.0 at 1 h and 45.7 ± 8.5 and 43.6 ± 8.2 at 3 h after administration. The filtered ^{99m}Tc -sulfur colloid %ID for the front and rear paws was 70.4 ± 11.0 and 66.3 ± 15.1 at 1 h and 55.5 ± 7.8 and 66.9 ± 8.5 at 3 h. Lymph node accumulation of each agent at either 1 or 3 h was not significantly different. **Conclusion:** ^{99m}Tc -DTPA-mannosyl-dextran is a receptor-based sentinel node radiotracer that exhibits the desired prop-

erties of rapid injection site clearance and low distal node accumulation. This molecule is the first member of a new class of diagnostic agents based on a macromolecular backbone with a high density of sites for the attachment of substrates and imaging reporters.

Key Words: sentinel node; ^{99m}Tc ; DTPA-mannosyl-dextran; receptor-binding radiopharmaceutical

J Nucl Med 2001; 42:951-959

When designing a receptor-targeted diagnostic agent, the fundamental goal is to deliver an adequate amount of imaging reporter per receptor. Progress in receptor-binding radiopharmaceuticals has been possible because radiotracers can be synthesized with specific activities that are compatible with typical target tissue receptor densities and detector sensitivities of PET and SPECT scanners. The development of MRI and CT receptor-binding agents has been challenging because of the decreased sensitivities of these modalities. One approach to this problem is to encapsulate or embed the reporter into a particle. An alternative is to attach multiple units of a reporter onto a molecular backbone that carries the receptor substrate. Proof-of-principle for this approach has been demonstrated for hepatocyte-specific MRI contrast enhancement (1) and receptor-targeted lymphoscintigraphy (2). The principal impediment to the development of these agents was the lack of an inexpensive molecular backbone with a high density of attachment sites for the receptor substrate and imaging reporter. The MRI agent requires a high density of attachment sites for gadolinium delivery to the limited number of hepatocyte receptors. The lymphoscintigraphy agent requires a high density of receptor substrate sites to achieve a receptor affinity required for proper sentinel node detection.

Sentinel node biopsy (3) is rapidly entering common practice for melanoma (4,5) and breast cancer (6-8). Although the technique has yet to be standardized (9), it is typically performed using a ^{99m}Tc -labeled colloid and a blue dye (10). The radiotracer is first used preoperatively to determine the location of the sentinel node and is then used intraoperatively to guide the dissection to the sentinel node. The blue dye, which has a very rapid transit through the lymph channels and nodes, is used to visually confirm the selection of the radioactive node as the sentinel lymph node.

Received Oct. 2, 2000; revision accepted Jan. 12, 2001.
For correspondence or reprints contact: David R. Vera, PhD, Radiology, 8756, 200 W. Arbor Dr., San Diego, CA 92103-8756.

One barrier to standardization is the fact that neither the blue dye nor any of the ^{99m}Tc -labeled agents have been designed for sentinel node detection or approved by the Food and Drug Administration for sentinel node detection. Consequently, these agents do not exhibit high sentinel node extraction. As a result, they travel to distal lymph nodes, which are detected as additional sentinel nodes. The following agents (11,12) are in current use for sentinel node detection: ^{99m}Tc -sulfur colloid, filtered ^{99m}Tc -sulfur colloid, ^{99m}Tc -antimony trisulfide, and various preparations of ^{99m}Tc -labeled albumin microcolloids. None of these agents exhibit ideal properties of both rapid injection site clearance and high sentinel node extraction. Consistent with this lack of standardization is the consensus that sentinel node detection has a long learning curve and a wide range of reported false-negative rates, from 0% to 12% (13). We propose that a rationally designed sentinel node radiopharmaceutical will improve diagnostic performance.

In this article, we report the synthesis and testing of a ^{99m}Tc -labeled receptor-binding radiopharmaceutical that exhibits the biochemical properties required for sentinel node detection. These properties, small molecular diameter and high receptor affinity, yield a radiopharmaceutical with rapid injection site clearance and low distal lymph node accumulation. This report also introduces a scalable synthesis of a molecular backbone capable of delivering high densities of imaging reporters to specific receptors.

MATERIALS AND METHODS

Reagents

Pharmaceutical-grade dextran (PM10; weight average molecular weight, 9,500) was obtained from Amersham-Pharmacia Biotech (Piscataway, NJ). All aqueous solutions were prepared using deionized water (NANOpure Infinity; Barnstead/Thermolyne, Dubuque, IA). Dimethylsulfoxide was obtained as U.S. Pharmacopeia grade from Gaylord Chemical Corp. (Slidell, LA). Ammonium persulfate was purchased from Aldrich (Milwaukee, WI) at >99.99% purity and stored at 4°C. Cyanomethyl-2,3,4,6-tetra-*O*-acetyl-1-thio- β -D-mannoside (CNM-thiomannose) was synthesized by published methods (14–16). Methanol was obtained as American Chemical Society grade, stored over 4A molecular sieves, and distilled immediately before use. All dextran conjugates were lyophilized and stored at –80°C. Dextran standards (stored at –80°C) were prepared by dissolution in deionized water followed by lyophilization. Particle-size standards (National Institute of Standards and Technology/Bureau of Certified Reference-traceable) were purchased from Duke Scientific Corp. (Palo Alto, CA). All other reagents were purchased from commercial suppliers and used as received.

Synthesis

Amino-Terminated Leash Conjugation. The synthesis of DTPA-mannosyl-dextran started with the attachment of amino-terminated leashes to the hydroxyl units of dextran. This attachment was a 2-step process (Fig. 1). The first step was the activation of the dextran hydroxyl units with allyl bromine (17,18). This reaction, which used 10 g PM10 dextran in 75 mL deionized water, was performed at 50°C and pH 11 in the presence of sodium hydroxide

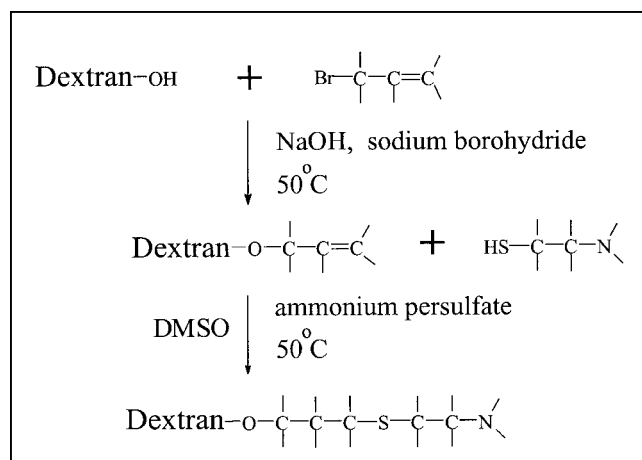


FIGURE 1. Covalent attachment of amino-terminated leashes to dextran hydroxyl groups is 2-step process, which prevents dextran cross-linking. DMSO = dimethyl sulfoxide.

(2.5 g) and sodium borohydride (0.2 g). The pH was maintained by dropwise addition of 2.5N NaOH. After 3 h, the solution was neutralized with acetic acid (2.5 mol/L) and the reaction was placed in a 5°C refrigerator for 2 h. After the top organic layer was decanted and 100 mL deionized water were added, the resulting solution was filtered (5 μm) into an ultrafiltration cell and diafiltered (molecular weight cutoff, 3,000) with 10 exchange volumes of deionized water. The product, allyl-dextran, was then concentrated and lyophilized.

In the second step, the allyl-dextran was reacted with 7.5 g aminoethanethiol in dimethylsulfoxide (30 mL) to produce an amino-terminated conjugate. This reaction was initiated with ammonium persulfate (1.0 g) and was performed under a nitrogen atmosphere. After 3 h, the reaction volume was doubled with deionized water, the solution was adjusted to pH 4 with sodium hydroxide (2.5N), and the product was diluted with 140 mL sodium acetate buffer (0.02 mol/L, pH 4). The product was then filtered (5 μm) into an ultrafiltration cell and dialyzed with 5 exchange volumes of acetate buffer (0.02 mol/L, pH 4) followed by 5 exchange volumes of deionized water. After concentration, the amino-terminated dextran was lyophilized. A sample was then assayed for the average number of amino groups per dextran, which was defined as the amine density.

DTPA Conjugation. We used the mixed anhydride method (19) to conjugate (Fig. 2A) DTPA to the dextran backbone. Activation of DTPA (20 g) with isobutylchloroformate (3.1 mL) was performed in acetonitrile (83 mL) at –30°C. The activated DTPA was slowly added to the amino-terminated dextran (2 g) in bicarbonate buffer (0.1 mol/L, pH 9). This solution was stirred overnight at room temperature. After diafiltration of the product with 5 exchange volumes of bicarbonate buffer (0.1 mol/L, pH 9) followed by 5 exchange volumes of deionized water, the retentate was concentrated and lyophilized. A sample was then assayed for DTPA and amine densities.

Mannose Conjugation. DTPA-dextran was conjugated with mannose by imidate coupling (Fig. 2B). Immediately before mannosyl conjugation, this product was deacetylated with sodium methoxide (0.05 mg/mL) in dry, freshly distilled methanol (250 mL) using a CNM-thiomannose concentration of 0.04 g/mL of methanol (16). After removal of the methanol by rotary evapora-

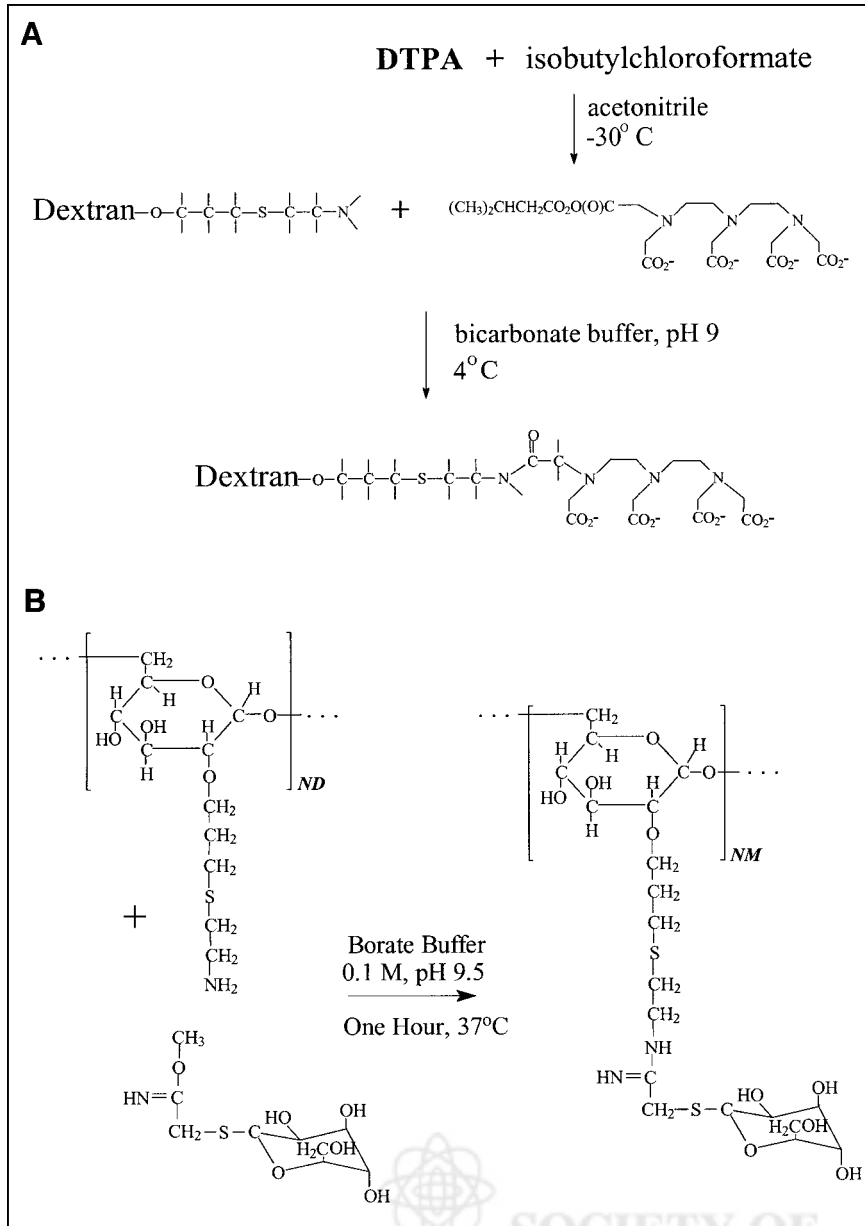


FIGURE 2. Attachment to amino-terminated leashes of chelator, DTPA (A), and receptor substrate, mannose (B).

tion, the coupling reaction was performed by the addition of an appropriate amount of DTPA-dextran (0.5 g) in a 20 mg/mL solution of Clarks borate buffer (0.2 mol/L, pH 9.0). The reaction was conducted at room temperature for 2 h. After filtration (5 μm), the product was transferred into an ultrafiltration cell and dialyzed with 5 exchange volumes of bicarbonate buffer (0.1 mol/L, pH 9) followed by another 5 exchange volumes of deionized water, and the retentate was concentrated and lyophilized. A sample was then assayed for mannose, DTPA, and amine densities.

Measurement of Amine Density. The average number of amino groups per dextran was measured in the following manner. The lyophilized dextran conjugate was dissolved in saline, and the amine concentration was measured by the trinitrobenzene sulfonate assay (20) using hexylamine as a standard. The glucose concentration of the same sample was measured by the sulfuric acid method (21). The amino density was calculated by dividing the amine concentration by the glucose concentration followed

by multiplication by the average number of glucose units per dextran.

Measurement of DTPA Density. The average number of DTPA units per dextran was measured after complexation of the DTPA conjugate with gadolinium. Lyophilized DTPA-dextran was dissolved in 0.1 mmol/L triethanolamine HCl (pH 6.0). To the DTPA conjugate solution, we added a 50% excess of gadolinium (mol/mol with respect to DTPA) as a 66 mmol/L solution (filtered, 0.2 μm) of 0.1N HCl and then adjusted the pH to 6 with 2.5N NaOH. After the solution was stirred for 24 h at 37°C, it was transferred to an Amicon ultrafiltration system (Millipore, Bedford, MA) for diafiltration at a molecular weight cutoff of 3,000 Da. After diafiltration with 10 exchange volumes of deionized water followed by another 10 exchange volumes of acetate buffer (0.2 mol/L, pH 4), the retentate was concentrated and assayed for gadolinium concentration by inductively coupled plasma spectrometry (1). The glucose concentration of the same sample was also measured by

the sulfuric acid method (21). The DTPA density was calculated by dividing the gadolinium concentration by the glucose concentration followed by multiplication by the average number of glucose units per dextran.

Measurement of Mannose Density. The average number of mannose groups per dextran was calculated in the following manner. The lyophilized dextran conjugate was dissolved in triethanolamine and labeled with gadolinium as described above. After diafiltration and measurement of DTPA concentration, the mannose concentration of the same sample was also measured by the sulfuric acid method (21). The mannose density was calculated by dividing the mannose concentration by the dextran concentration, which was calculated on the basis of the known DTPA density of the DTPA-dextran conjugate.

Measurement of Size Distribution. The mean diameter of each conjugate was measured by dynamic light scattering (UPA-150; Honeywell-Microtrac, Clearwater, FL). Each conjugate was assayed for 10 min at a concentration > 5 mg/mL of 0.9% saline. The refractive index of each sample was assayed (Fisher Scientific, Santa Clara, CA) and did not deviate from 0.9% saline (1.33). Latex particle standards of 3 different sizes gave weight-averaged diameters that were within 5% of their mean diameters (19 ± 1.5 , 102 ± 3 , and 993 ± 21 nm), which were calibrated by photon correlation spectroscopy or electron microscopy. The analyzer software did not assume a gaussian size distribution. Mean molecular diameters with SDs were calculated from volume distribution data.

Radiolabeling

^{99m}Tc-DTPA-Mannosyl-Dextran. Tin reduction was used to label DTPA-mannosyl-dextran with ^{99m}Tc. DTPA-mannosyl-dextran (1.5 mg, 0.41 nmol) was added to a 2-mL glass vial. The vial was capped with a silicone/polytetrafluoroethylene septum, and 0.5-mL sodium pertechnetate (approximately 0.75 GBq) was added. The vial was then purged for 10 min with filtered (0.22 μm) medical-grade nitrogen. During this time, a tin chloride solution was prepared by the addition of 0.175 mL HCl (37%) to 5.0 mg SnCl₂ followed by 25 mL 0.9% saline. Immediately after cessation of the nitrogen purge, 500 μL ascorbic acid (0.5 μmol/mL 0.9% saline) and 50 μL of the acidified saline solution of tin chloride were rapidly injected into the labeling vial. After the solution stood for 1 h at room temperature, 1.0 mL phosphate-buffered saline (pH 7.2, 0.1 mol/L phosphate, 0.15 mol/L chloride) was added to the labeling vial. The labeled product used in the biodistribution and in vitro binding studies was purified by size-exclusion chromatography (G-25SF, 1 × 9 cm; Amersham Pharmacia Biotech [1 mL/min 0.9% saline]). Standing gel chromatography (22) was performed by stopping the column flow at 1 min after injection and scanning (23) the column for radioactivity (100–200 keV). Chromatography of the unpurified product with Sephacryl S-300HR (1 × 30 cm; Amersham Pharmacia Biotech) was used to test for possible cross-linking; the mobile phase (1 mL/min 0.9% saline) was monitored by ultraviolet absorbance (226 nm) and radioactive detection (100–200 keV). The void volume of this column was calibrated with blue dextran (Sigma, St. Louis, MO). Instant thin-layer chromatography (ITLC) with 31ET media (Whatman, Ann Arbor, MI) and acetone was performed using standard technique (24). The concentration of the injectate was measured by ultraviolet spectrometry (226 nm) using known concentrations of DTPA-mannosyl-dextran as a standard curve.

Filtered ^{99m}Tc-Sulfur Colloid. ^{99m}Tc-labeled sulfur colloid was prepared from a commercial kit (CIS, Bedford, MA) using the labeling protocol specified by the package insert. A 3-mL volume of sodium pertechnetate (approximately 2 GBq) was used to reconstitute the thiosulfate vial. No attempt was made to optimize the filtration yield by adjusting the volumes of the kit components. A known activity of the product was passed through a 0.22-μm syringe filter (Millex GV; Millipore). After calculation of the filtration yield, the radiochemical purity of the filtered and unfiltered product was measured by ITLC (25) using type SG media (Gelman, Ann Arbor, MI) and 85% methanol. The developed stripes were cut at an R_f of 0.1 and assayed in a γ well counter (100–200 keV). The colloid yield was defined as the percentage of radioactivity at the origin (R_f < 0.1) (26). All doses of the filtered preparation were administered within 15 min of the filtration step.

In Vitro Binding Assay

The equilibrium dissociation constant for binding to rabbit liver was measured as previously described (27). Previous studies of the mannose-binding protein receptor (28) showed equivalent affinities for liver and lymph node binding. Briefly, DTPA-mannosyl-dextran was labeled with 2.2 GBq ^{99m}Tc, column purified, and diluted to 7 concentrations. ^{99m}Tc-DTPA-mannosyl-dextran at various concentrations (2.1×10^{-6} to 2.1×10^{-11} mol/L) was incubated with homogenized liver in 200 μL assay buffer (pH 7.5; 1.0 mol/L NaCl, 0.05 mol/L CaCl₂, 0.05 mol/L MgCl₂, 0.05 mol/L Tris-HCl, and 0.1% human serum albumin). The incubation was performed at 37°C for 30 min in uncapped polyallomer ultracentrifuge tubes (7 × 20 mm; Beckman Coulter, Inc., Fullerton, CA) on a hematology mixer (Fisher Scientific) that provided both rocking and rotation. Bound and free activity were separated by ultracentrifugation (Optima TLX; Beckman Coulter) for 20 min at 75,000 rpm (TLA-100 rotor; Beckman Coulter). After 2 washes with 200 μL buffer, the empty ultracentrifuge tube and the washings were placed in separate plastic scintillation vials and assayed for radioactivity (100–200 keV). The computer program LIGAND (National Institutes of Health, Bethesda, MD) (29) was used to calculate the equilibrium dissociation constant, K_D; the receptor concentration, [R]; and N₁, a ratio that represents the amount of nonspecifically bound ligand.

Biodistribution

Preliminary biodistribution of ^{99m}Tc-DTPA-mannosyl-dextran was assessed in New Zealand White rabbits. These studies were performed under a protocol approved by the Institutional Animal Care and Use Committee. After anesthesia with an intramuscular injection of ketamine and xylazine, ^{99m}Tc-DTPA-mannosyl-dextran (0.050 mL, 0.22 nmol, approximately 3.7 MBq) or filtered ^{99m}Tc-sulfur colloid (0.050 mL, approximately 3.7 MBq) was injected into all 4 foot pads. Four rabbits (2.5–3.0 kg) were studied at each time point with each agent. All rabbits received only 1 radiotracer. After injection, each foot pad was massaged for 1 min, with a 10 × 10 cm (4 × 4 inch) gauze pad placed between the injection site and a gloved thumb. At 55 or 175 min after injection, 0.050 mL isosulfan blue 1% (U.S. Surgical Corp., Norwalk, CT) was administered to each foot pad. Five minutes after the isosulfan blue injection, each animal was euthanized by a barbiturate overdose under anesthesia. The paws and the popliteal, axillary, and iliac lymph nodes were excised and assayed for radioactivity (100–200 keV) with 0.0050-mL samples (cpm_{standard}) of the ^{99m}Tc-DTPA-mannosyl-dextran dose. We also assayed each gauze pad for radioactivity. If the pad contained more than 2% of the dose,

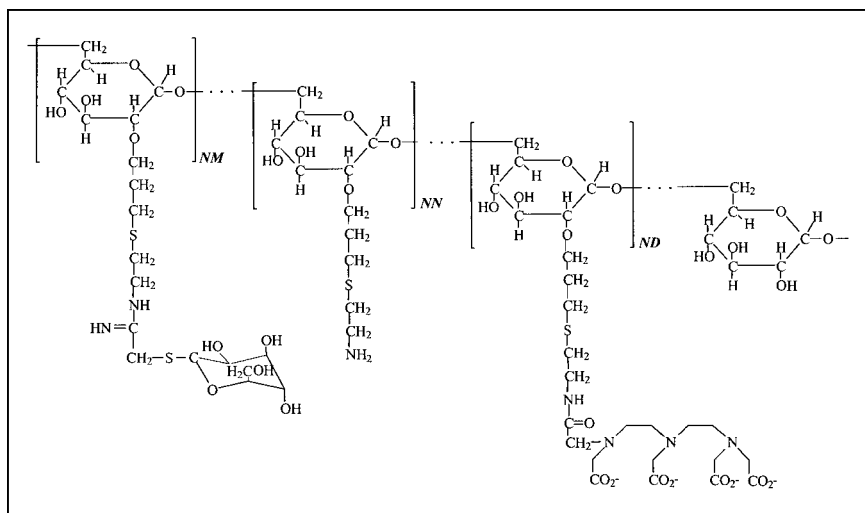


FIGURE 3. DTPA-mannosyl-dextran amine (NN), mannose (NM), and DTPA (ND) densities were 23, 55, and 8 mol per dextran. Average molecular weight was 35,800 g/mol, and mean molecular diameter was 7.1 nm.

we considered the injection a misadministration and did not include the injection site and corresponding lymph node data in the study. The percentage injected dose (%ID) for the front and rear injection sites and the axillary, popliteal (%ID_{popliteal}), and iliac (%ID_{iliac}) lymph nodes was calculated as:

$$\%ID = \text{cpm}_{\text{tissue}} \times 100 / (\text{cpm}_{\text{standard}} \times 10). \quad \text{Eq. 1}$$

The popliteal extraction, PE, was calculated as:

$$PE = (\%ID_{\text{popliteal}} - \%ID_{\text{iliac}}) \times 100 / \%ID_{\text{popliteal}}. \quad \text{Eq. 2}$$

Statistical Analysis

Values are presented as mean \pm SD. The significance of differences between $^{99\text{m}}\text{Tc}$ -DTPA-mannosyl-dextran and filtered $^{99\text{m}}\text{Tc}$ -sulfur colloid was determined using the Student *t* test for paired data. The program (JMP; SAS Institute Inc., Cary, NC) assumed equal variances; $P < 0.05$ was considered statistically significant.

RESULTS

Synthesis

The unlabeled product, DTPA-mannosyl-dextran (Fig. 3), had a molecular weight of 35,800 g/mol and a molecular diameter of 7.1 ± 0.9 nm. The final amino, mannose, and DTPA densities were 23, 55, and 8 moles per dextran. Table 1 lists the coupling densities, molecular weights, and mo-

lecular diameters for PM10 dextran, each intermediate conjugate, and the final product, DTPA-mannosyl-dextran.

Radiolabeling

Labeling yields were in excess of 98% and stable for 6 h. Specific activities of 74×10^6 GBq/mol were achieved. Figure 4 is a typical standing gel chromatogram, which demonstrated an absence of reduced, hydrolyzed $^{99\text{m}}\text{Tc}$ at the top of the 8-cm Sephadex column. Figure 5 is a typical absorbance and radioactivity profile of fast protein liquid chromatography performed 6 h after labeling. This chromatogram demonstrated an absence of polymeric dextran, which would be detected by the absorbance profile at the column void volume (V_0), and unbound $^{99\text{m}}\text{Tc}$, which would be detected by the radioactivity profile at the bed volume. The percentage bound measurements through ITLC showed high $^{99\text{m}}\text{Tc}$ -DTPA-mannosyl-dextran labeling stability for at least 6 h (Fig. 6A) and an approximately 10% loss in percentage bound after $^{99\text{m}}\text{Tc}$ -sulfur colloid filtration (Fig. 6B).

In Vitro Binding

The equilibrium dissociation constant for binding to the mannose-terminated glycoprotein receptor was 0.12 ± 0.07 nmol/L. The specific binding data are graphed in Figure 7 in

TABLE 1
Molecular Parameters

Conjugate	Coupling density (mol/dextran)				Weight (g/mol)	Diameter* (nm)
	Allyl	Amine	DTPA	Mannose		
Dextran					9,500	4.0 ± 0.5
Allyl-dextran	86				13,000	7.3 ± 1.2
Amino-dextran		86			19,600	8.8 ± 0.9
DTPA-dextran		78	8		22,800	7.2 ± 1.8
DTPA-mannosyl-dextran		23	8	55	35,800	7.1 ± 0.9

*Mean \pm SD.

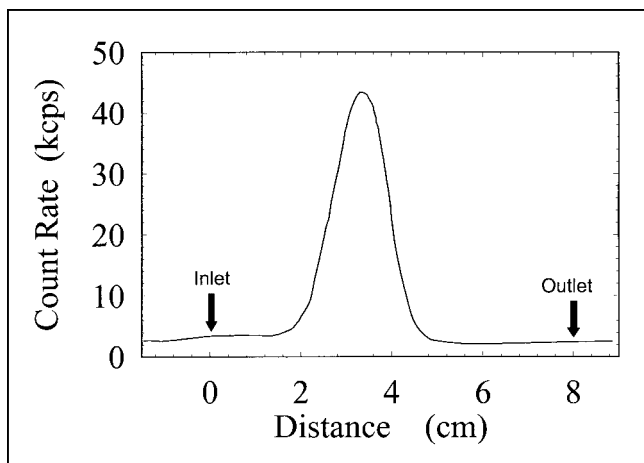


FIGURE 4. Standing gel chromatography of ^{99m}Tc -DTPA-mannosyl-dextran showed absence of reduced unbound ^{99m}Tc .

the Scatchard form. Each symbol represents a data point corrected for nonspecific binding by N1, which equaled 0.273 ± 0.011 . The Scatchard line was calculated by LIGAND and yielded an x -axis intercept of 0.116 ± 0.074 nmol/L, which is the receptor concentration.

Biodistribution

Tables 2 and 3 list the %ID at 1 and 3 h, respectively, for the axillary, popliteal, and iliac lymph nodes, the %ID for the injection sites at the front and rear foot pads, and the popliteal extraction. The maximum number of injection sites and axillary or popliteal lymph nodes at each time point was 8. Axillary, popliteal, and iliac lymph node accumulations at 1 h were not significantly different for filtered ^{99m}Tc -sulfur colloid and ^{99m}Tc -DTPA-mannosyl-dextran. None of the lymph nodes exhibited a statistically significant change in %ID between the 1- and 3-h time points. The popliteal extraction at both 1 h and 3 h was significantly ($P < 0.05$) higher for ^{99m}Tc -DTPA-mannosyl-dextran (90.1 ± 10.7 and 97.7 ± 2.0 %ID, respectively) than for filtered ^{99m}Tc -sulfur colloid (78.8 ± 6.5 and $67.4 \pm$

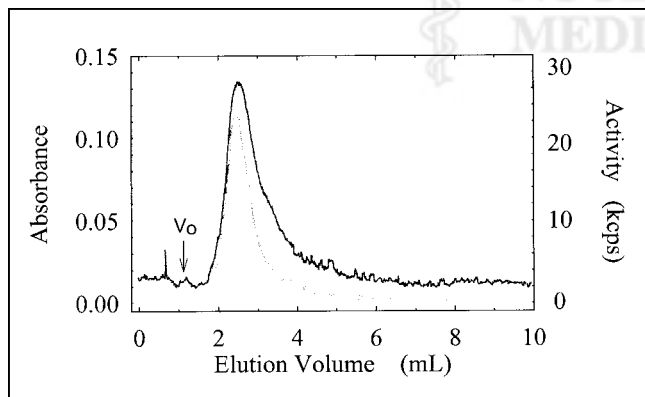


FIGURE 5. Fast protein liquid chromatography 6 h after labeling showed absence of polymeric dextran and unbound ^{99m}Tc (absorbance, black line; activity, gray line). V_0 = void volume.

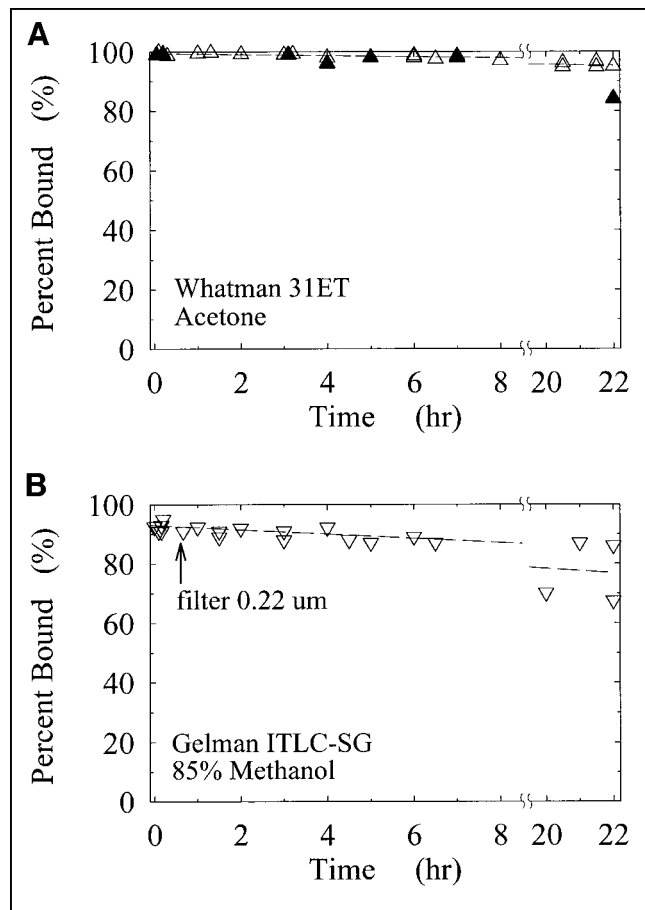


FIGURE 6. Percentage bound measurements through ITLC showed high ^{99m}Tc -DTPA-mannosyl-dextran labeling stability for at least 6 h (A) and approximately 10% loss in percentage bound after ^{99m}Tc -sulfur colloid filtration (B). B contains results of 3 labeling experiments. Δ = ITLC results from 4 labeling experiments without purification; \blacktriangle = ITLC results from G-25SF-purified ^{99m}Tc -DTPA-mannosyl-dextran.

26.8 %ID, respectively). ^{99m}Tc -DTPA-mannosyl-dextran exhibited significantly faster injection site clearance than did filtered ^{99m}Tc -sulfur colloid. The ^{99m}Tc -DTPA-mannosyl-dextran %ID for the front and rear paws was 52.6 ± 10.5 and 52.3 ± 8.0 at 1 h and 45.7 ± 8.5 and 43.6 ± 8.2 at 3 h after administration. The filtered ^{99m}Tc -sulfur colloid %ID for the front and rear paws was 70.4 ± 11.0 and 66.3 ± 15.1 at 1 h and 55.5 ± 7.8 and 66.9 ± 8.5 at 3 h. Axillary and popliteal accumulation at either 1 or 3 h was not significantly different between agents.

DISCUSSION

Our results demonstrate the receptor-binding properties of a radiolabeled mannosyl-neoglycoconjugate based on a highly substituted dextran backbone. These properties are receptor specificity and affinity as exhibited by the in vitro binding assay. The biodistribution data demonstrated faster injection site clearance and lower distal lymph node accumulation than were seen for a nonreceptor-targeted particle,

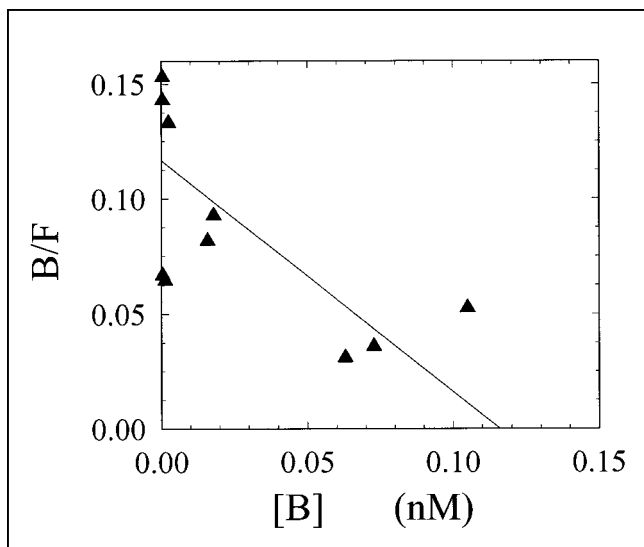


FIGURE 7. In vitro assay of ^{99m}Tc -DTPA-mannosyl-dextran binding to liver measured equilibrium dissociation constant, K_D , of 0.12 ± 0.07 nmol/L. [B] = bound concentration; B/F = bound-to-free ratio.

filtered ^{99m}Tc -sulfur colloid. These features, which are highly desirable for a sentinel node agent, can be rationally controlled by selection of the molecular weight of the dextran and the mannose density of the neoglycoconjugate.

Our biodistribution studies did not demonstrate a significant difference in sentinel node uptake between the receptor-binding agent and filtered ^{99m}Tc -sulfur colloid. Increased uptake would be a minor benefit if the injection site clearance remained unchanged. For example, if the sentinel node uptake were to double from 5 to 10 %ID, the injection site of a particulate agent would change from 95% to 90% of the dose. The solution is to provide 2 routes by which the agent may clear the injection site. Using a small- to medium-size molecule that binds to the sentinel node through a biochemical interaction permits a second route of clearance through diffusion into the blood capillaries. This strategy does have a disadvantage in that this agent, once in the blood, will accumulate in the liver and urine. Given the distance of the

liver and urinary bladder from the axillary basin, we do not foresee any interference with sentinel node imaging or intraoperative detection in breast cancer patients. Lastly, the SDs of some of the lymph node measurements are higher than those of typical biodistribution data resulting from intravenous injections. We attribute this difference to biologic variation in lymph node drainage of the foot pads; for this reason, we used 4 rabbits per agent at each time point, which yielded up to 8 axillary and 8 popliteal lymph nodes for each time point.

Our choice of dextran as the molecular backbone was based on practicality and availability. Previous studies with receptor-targeted MRI (1), in vitro receptor assays (27), and sentinel node detection (2) used polylysine as the molecular backbone. Although these studies showed proof-of-principle, clinical implementation based on polylysine was not feasible. Polylysine is expensive and has a small clinical database. Dextran is inexpensive and has a well established safety record (30,31). More important, dextran is available in a wide selection of molecular weights. Additionally, dextran is very hydrophilic, a property that promotes injection site clearance (32). Alternatives such as starburst dendrimers (33) or polylysine (1) are 10-fold the cost per gram. Additionally, amine-terminated dendrimers exhibited poor biocompatibility and anionic dendrimers displayed significant liver uptake (34). Another important aspect is the direct observation (35) that the interstitial diffusion coefficient for neutral dextrans is 10-fold greater than that for proteins of the same hydrodynamic radius. This property was attributed to the greater hydrophilicity and flexibility of the dextran, as well as the absence of charge, the presence of which reduces migration across charged membrane structures. Consequently, dextran conjugates, if properly designed, will deliver a greater density of reporter atoms than do rigid or charged structures.

We consider the ability to control the molecular weight of this agent to be a critical feature of our design strategy. By selecting a dextran from the various molecular weights and controlling the number of substrate and reporter groups

TABLE 2
Biodistribution at 1 Hour

Agent	%ID					
	Lymph nodes			Injection sites		Popliteal extraction* (%)
	Axillary	Popliteal	Iliac	Front	Rear	
^{99m}Tc -DTPA-mannosyl-dextran	4.0 ± 3.7	6.1 ± 4.5	0.75 ± 0.88	52.6 ± 10.5	52.3 ± 8.0	90.1 ± 10.7
Filtered ^{99m}Tc -sulfur colloid	5.4 ± 2.7	4.8 ± 1.5	0.94 ± 0.19	70.4 ± 11.0	66.3 ± 15.1	78.8 ± 6.5
$n_{\text{TcDx}}/n_{\text{TcSC}}^\dagger$	7/8	8/6	4/3	7/7	8/7	8/6
<i>P</i>	0.42	0.48	0.73	<0.01	0.039	0.042

* $(\%ID_{\text{popliteal}} - \%ID_{\text{iliac}}) \times 100 / \%ID_{\text{popliteal}}$.

† Number of lymph nodes or injection sites for each agent (^{99m}Tc -DTPA-mannosyl-dextran [TcDx] or filtered ^{99m}Tc -sulfur colloid [TcSC]) at each time point that satisfied our injection criteria.

TABLE 3
Biodistribution at 3 Hours

Agent	%ID					Popliteal extraction* (%)
	Lymph nodes			Injection sites		
	Axillary	Popliteal	Iliac	Front	Rear	
^{99m} Tc-DTPA-mannosyl-dextran	6.1 ± 10.7	6.1 ± 5.5	0.18 ± 0.24	45.7 ± 8.5	43.6 ± 8.2	97.7 ± 2.0
Filtered ^{99m} Tc-sulfur colloid	6.2 ± 2.2	6.0 ± 3.3	2.17 ± 2.70	55.5 ± 7.8	66.9 ± 8.5	67.4 ± 26.8
n _{TcDx} /n _{TxSC} [†]	7/8	8/8	4/4	7/8	8/8	8/8
P	0.98	0.97	0.19	0.036	<0.001	0.007

* $(\%ID_{\text{popliteal}} - \%ID_{\text{iliac}}) \times 100 / \%ID_{\text{popliteal}}$.

[†]Number of lymph nodes or injection sites for each agent (^{99m}Tc-DTPA-mannosyl-dextran [TcDx] or filtered ^{99m}Tc-sulfur colloid [TcSC]) at each time point that satisfied our injection criteria.

attached to the dextran, we can tailor the size of the agent to the imaging problem. For sentinel node detection, we selected PM10 dextran, which has an average molecular weight of 9,500 and a mean diameter of 4.6 nm. After attachment of 55 mannose and 8 DTPA groups, the resulting molecular weight and diameter were 35,800 g/mol and 7.1 nm. Our intention was to design a radiopharmaceutical of moderate size. A linear molecule of 7.1 nm would promote injection site clearance by permitting entrance into both the blood and the lymph capillaries. Our hypothesis is that radiation scattered from the injection site controls the tissue background observed by the surgeon during intraoperative detection. Consequently, a radiotracer that clears more rapidly from the injection site, even if the radiotracer delivers equal activity to the sentinel node, will provide better detection (a higher signal-to-background ratio) than will an agent with slower clearance.

A second design goal was to obtain a radiotracer of ultrahigh receptor affinity. Our intention was to obtain an agent with 100% extraction by the lymph node. The equilibrium dissociation constant of 0.12 nmol/L ranks this preparation of ^{99m}Tc-DTPA-mannosyl-dextran among the most avid of the labeled neoglycoconjugates. Dissociation constants for other labeled neoglycoconjugates are 0.33 nmol/L for ^{99m}Tc-DTPA-galactosyl-polylysine (27), composed of 185 biantennary galactose units and 24 DTPA groups attached to a backbone of 120 lysines; 0.14 nmol/L for iodine-labeled galactosyl-neoglycoalbumin, with a galactose density of 44 mol/mol (36); and 0.19 nmol/L for gallium-labeled deferoxamine-neoglycoalbumin, with a galactose density of 41 mol/mol (37).

Our selection of DTPA as the chelation system was based on clinical experience with this system. Two commercial kits using DTPA-albumin exist in Japan, ^{99m}Tc-DTPA-albumin and ^{99m}Tc-DTPA-galactosyl-neoglycoalbumin (38). The former agent exhibited a plasma clearance equivalent to that of ¹³¹I-albumin (39). We are aware of the consensus that the nitrogen-sulfur tetradentate chelates afford more stable

chelation then does conjugated DTPA. The basis for this generalization comes mainly from the literature on radiolabeled antibodies. To our knowledge, the only direct comparison of a conjugated DTPA with an N_xS_y system demonstrated equivalent stability to a cysteine challenge (40).

Finally, the reaction scheme will provide an opportunity to design receptor-targeted agents for MRI and possibly CT. Although the biochemistry literature is replete with methods for the attachment of small molecules to dextran-based chromatography media, these techniques result in attachments to a very small fraction of the glucose units. Delivery of an adequate number of reporter units per receptor will require a high density of attachment sites. The dextran conjugate used in this study consisted of 1.5 attachment sites per glucose unit. The essential feature of the reaction scheme was the use of a 2-step process that used a heterobifunctional reagent, cysteamine, to create the amino-terminated leash. This process eliminated the possibility of cross-linking and allowed the reaction to be performed at high dextran concentrations. Our long-term goal is to apply the receptor-based pharmacokinetic modeling developed by nuclear imaging to MRI and CT observations of regional tissue biochemistry.

CONCLUSION

^{99m}Tc-DTPA-mannosyl-dextran is the first member of a new class of receptor-targeted diagnostic agents based on a macromolecular backbone with a high density of sites for the attachment of receptor substrates and imaging reporters. This radiopharmaceutical is the first specifically designed for sentinel node detection and exhibits the desired properties of rapid injection site clearance and low distal node accumulation. Our long-term goal is to increase the diagnostic performance of the sentinel node technique. The result would be a wider dissemination, beyond academic centers, and greater access for patients with breast cancer or melanoma.

ACKNOWLEDGMENTS

The authors thank Neoprobe Corp., Dublin, OH, for the use of a model 1000 portable radioisotope detector and Amersham-Pharmacia Biotech for the generous gift of PM10 dextran. This study was supported in part by National Cancer Institute grant CA72751 and University of California Breast Cancer Research Program grants 2RB-0018 and 4IB-0051.

REFERENCES

1. Vera DR, Buonocore MH, Wisner ER, Katzberg RW, Stadalnik RC. A molecular receptor-binding contrast agent for magnetic resonance imaging of the liver. *Acad Radiol.* 1995;2:497–507.
2. Vera DR, Wisner ER, Stadalnik RC. Sentinel node imaging via a nonparticulate receptor-binding radiotracer. *J Nucl Med.* 1997;38:530–535.
3. Morton DL, Wen D-R, Wong JH, et al. Technical details of intraoperative lymphatic mapping for early stage melanoma. *Arch Surg.* 1992;127:392–399.
4. Glass LF, Messina JL, Cruse W, et al. The use of intraoperative radiolymphoscintigraphy for sentinel node biopsy in patients with malignant melanoma. *Dermatol Surg.* 1996;22:715–720.
5. Gershenwald JE, Tseng C-H, Thompson W, et al. Improved sentinel lymph node localization in patients with primary melanoma with the use of radiolabeled colloid. *Surgery.* 1998;124:203–210.
6. Giuliano AE, Kirgan DM, Guenther JM, Morton DL. Lymphatic mapping and sentinel lymphadenectomy for breast cancer. *Ann Surg.* 1994;220:391–401.
7. Albertini JJ, Cruse CW, Rapaport D, et al. Intraoperative radiolymphoscintigraphy improves sentinel lymph node identification for patients with melanoma. *Ann Surg.* 1996;223:217–224.
8. Krag DN, Weaver D, Ashikaga T, et al. The sentinel node in breast cancer: a multicenter validation study. *N Engl J Med.* 1998;339:941–946.
9. Keshtgar MRS, Ell PJ. Sentinel lymph node detection and imaging. *Eur J Nucl Med.* 1999;26:57–67.
10. Hirsch JJ, Tisnado J, Cho SR, Beachley MC. Use of isosulfan blue for identification of lymphatic vessels: experimental and clinical evaluation. *AJR.* 1982;139:1061–1064.
11. Alazraki NP, Eshima D, Eshima LA, et al. Lymphoscintigraphy, the sentinel node concept and the intraoperative gamma probe in melanoma, breast cancer and other potential cancers. *Semin Nucl Med.* 1997;27:55–68.
12. Wilhelm AJ, Mijnhout S, Franssen EJF. Radiopharmaceuticals in sentinel lymph node detection: an overview. *Eur J Nucl Med.* 1999;26:S36–S42.
13. Haigh PI, Giuliano AE. Role of sentinel lymph node dissection in breast cancer. *Ann Med.* 2000;32:51–56.
14. Kőrösy F, Bárczai-Martos M. Preparation of acetobrome-sugars. *Nature.* 1950;165:369.
15. Chipowsky S, Lee YC. Synthesis of 1-thioaldosides having an amino group at the aglycon terminal. *Carbohydr Res.* 1973;31:339–346.
16. Lee YC, Stowell CP, Krantz MJ. 2-Imino-2-methoxyethyl-1-thioglycosides: new reagents for attaching sugars to proteins. *Biochemistry.* 1976;15:3956–3963.
17. Holmberg A, Meurling L. Preparation of sulfhydrylborane-dextran conjugates for boron neutron capture therapy. *Bioconjug Chem.* 1993;4:570–573.
18. Gedda L, Olsson P, Ponten J, Carlsson J. Development and in vitro studies of epidermal growth factor-dextran conjugates for neutron capture therapy. *Bioconjug Chem.* 1996;7:584–591.
19. Krejcarek GE, Tucker KL. Covalent attachment of chelating groups to macromolecules. *Biochem Biophys Res Commun.* 1977;77:581–583.
20. Fields R. The rapid determination of amino groups with TNBS. *Methods Enzymol.* 1972;25:464–468.
21. Dubios M, Gilles KA, Hamilton JK, et al. Colorimetric method for determination of sugars and related substances. *Anal Chem.* 1956;28:350–356.
22. Persson BRR, Darte L. Gel chromatography column scanning for the analysis of Tc-99m-labelled compounds. *J Chromatogr.* 1974;101:315–326.
23. Jansholt A-L, Krohn KA, Vera DR, Hines HH. Radiochemical quality control using an inexpensive radiochromatogram scanner with analog and digital output. *J Nucl Med Technol.* 1980;8:222–227.
24. Kelly WN, Ice RD. Pharmaceutical quality of technetium-99m sulfur colloid. *Am J Hosp Pharm.* 1973;30:817–820.
25. Technetium Tc-99m sulfur colloid injection. In: *The United States Pharmacopeia.* Rockville, MD: The United States Pharmacopeial Convention; 1999:1602–1603.
26. Robbins PJ. *Chromatography of Technetium-99m Radiopharmaceuticals: A Practical Guide.* New York, NY: The Society of Nuclear Medicine; 1984.
27. Vera DR, Topcu S, Stadalnik RC. In vitro quantification of asialoglycoprotein receptor density from human hepatic microsomes. *Methods Enzymol.* 1995;247:394–402.
28. Kawasaki T, Mizuno Y, Masuda T, Yamashina I. Mannan-binding protein in lymphoid tissues of rats. *J Biochem (Tokyo).* 1980;88:1891–1894.
29. Munson PJ, Rodbard D. Ligand: a versatile computerized approach for characterization of ligand-binding systems. *Anal Biochem.* 1980;107:220–239.
30. Thoren L. Dextran as a plasma volume substitute. In: Jamieson GA, Greenwalt TJ, eds. *Blood Substitutes and Plasma Expanders.* New York, NY: Alan R Liss; 1978:265–282.
31. de Belder D. Medical application of dextran and its derivatives. In: Dumitriu S, ed. *Polysaccharides in Medicinal Applications.* New York, NY: Marcel Dekker; 1996:505–524.
32. Porter CJH. Drug delivery to the lymphatic system. *Crit Rev Ther Drug Carrier Syst.* 1997;14:333–393.
33. Tomalia DA, Baker H, Deward J, et al. A new class of polymers: starburst-dendritic macromolecules. *Polymer J.* 1985;17:117–132.
34. Malik N, Wiwattanapatapee R, Klopsch R, et al. Dendrimers: relationship between structure and biocompatibility in vitro, and preliminary studies on the biodistribution of ¹²⁵I-labelled polyamidoamine dendrimers in vivo. *J Controlled Release.* 2000;65:133–148.
35. Nugent J, Jain RK. Extravascular diffusion in normal and neoplastic tissues. *Cancer Res.* 1984;44:238–244.
36. Vera DR, Krohn KA, Stadalnik RC, Scheibe PO. Tc-99m galactosyl-neoglycoalbumin: in vitro characterization of receptor-mediated binding. *J Nucl Med.* 1984;25:779–787.
37. Vera DR. Gallium-labeled deferoxamine-galactosyl-neoglycoalbumin: a radiopharmaceutical for regional measurement of hepatic receptor biochemistry. *J Nucl Med.* 1992;33:1160–1166.
38. Torizuka K, Kawa S, Kudo M, et al. Phase III multi-center clinical study on ^{99m}Tc-GSA, a new agent for imaging of liver function. *Jap J Nucl Med.* 1991;29:159–181.
39. Shirakami Y, Matsumura Y, Yamamichi Y, Kurami M, Ueda N, Hazue M. Development of Tc-99m-DTPA-HSA as a new blood pool agent. *Jap J Nucl Med.* 1987;24:475–478.
40. Qu T, Wang Y, Zhu Z, Rusckowski M, Hnatowich DJ. Different chelators and different peptides together influence the in vitro and mouse in vivo properties of ^{99m}Tc. *Nucl Med Commun.* 2001;22:203–215.